

Research Article

SYNTHESIS, CHARACTERIZATION AND AMELIORATING EFFECT OF QUERCETIN NANOPARTICLES AGAINST ETHION-INDUCED OXIDATIVE STRESS IN MALE RATS

Ranjith D¹, Dhaval J Kamothi¹, Madhu CL¹, Padhi PK¹, Dinesh Kumar¹, Telang AG^{2*}

Received 28 April 2023, revised 22 November 2023

ABSTRACT: Pesticides are the ubiquitous xenobiotics. Ethion, an organophosphorus pesticide, induces adverse effects in animals upon ingestion. Quercetin, a potent antioxidant, has very low water solubility. As a result, this study aimed to synthesize and analyze nanoparticles of quercetin and assess their potential to mitigate oxidative harm caused by ethion in rats. Ethion was administered at dose rates of 3.6 and 7.2 mg/kg once daily for 90 days. Quercetin (50 mg/kg) and quercetin nanoparticles (50 mg/kg) were also simultaneously administered to high-dose ethion-administered rats in separate groups for 90 days. A 10% blood hemolysate was prepared and analyzed for different biochemical parameters. Groups subjected to ethion treatment exhibited a notable increase in lipid peroxidation, indicated by heightened MDA production, alongside a significant reduction in SOD levels, Catalase, GSH, GPX, GST, and GR. In groups treated with quercetin and quercetin nanoparticles, the impact of ethion-induced oxidative stress was notably mitigated, particularly in the quercetin nanoparticles-treated group.

Keywords: Pesticide, Ethion, Oxidative Stress, Quercetin, Quercetin nanoparticles.

INTRODUCTION

The endless advancement of the world population has created gigantic pressure to appease the universal need for products in agriculture. The major demand includes fertility of soil, natural soil depreciation by transforming to agricultural ecosystems, and creating arthropod resistance against traditional insecticidal preparations [1]. Insecticides are used to encounter insect pests, essentially to improve the production of agricultural products. The most common form of insecticides used in the agricultural sector includes organophosphates, organochlorines, carbamates, and pyrethroids act against the enzymatic system of arthropods [2]. Among the insecticides, organophosphates are the most used, and their toxicity remains a considerable cause of mortality and morbidity in third-world countries their regular use leads to residues in crops and may harm humans and animals [3]. The inadvertent and continual use of organophosphate insecticides engendered environmental

dissemination exerting a deleterious effect on biological systems through instigating oxidative damage [4].

Ethion, classified within the organophosphate pesticide category, was officially registered in the United States back in 1965 [5], a non-systemic pesticide and an acaricide used in fruit trees *viz.*, nut and citrus trees, forage crops, seeds and cotton including multitudinal fruits and vegetables [6]. As a result of worldwide use and easy availability of ethion, its use has become ubiquitous both in developed and developing countries, accelerating considerable public health hazards [7]. Administration of ethion will cause histopathological alterations and induction of oxidative stress in rats [8, 9].

Quercetin recognized as a potent scavenger of free radicals and a chelator of metals, is commonly found in various sources such as vegetables, grape wine, citrus fruits, parsley, and grains, boasting widespread distribution [10] and has predominant anti-inflammatory, antioxidant, and antibiotic activities [11].

¹Division of Pharmacology and Toxicology, ICAR-Indian Veterinary Research Institute, Izatnagar 243122, India.

²CADRAD, ICAR-Indian Veterinary Research Institute, Izatnagar 243122, India.

*Corresponding author. e-mail: agtelang@rediffmail.com

Furthermore, quercetin exhibits the capability to safeguard tissues against oxidative stress triggered by organophosphate pesticides [12]. However, due to its hydrophobicity and low bioavailability, quercetin has limited clinical application [13]. Consequently, an efficient method of quercetin delivery could be a useful strategy. The utilization of nano drug delivery systems offers advantages such as enhanced stability, greater capacity for carriers, facilitation of hydrophobic drug delivery, and sustained release of drugs. These systems also offer versatility in administration routes, encompassing oral intake and inhalation [14]. Different nanomaterials have been studied for their antioxidant activities in recent times [15,16,17]. The antioxidants can prevent or slow down the detrimental processes of oxidation inside the cells by removing free radicals [17, 18, 19]. Therefore, in the present study, the quercetin nanoparticles were synthesized by the ionic gelation method and evaluated for their ameliorating potential. This study aimed to demonstrate the impact of ethion on serum biochemical markers, parameters related to oxidative stress, and the potential mitigation offered by quercetin nanoparticles in Wistar albino rats over a 90-day treatment period.

MATERIALS AND METHODS

Chemicals and reagents

Ethion (technical grade) was purchased from Cheminova Industries Ltd, and Quercetin was obtained from Merck Pharmaceuticals (Mumbai, India). Chitosan and Sodium Tri Poly Phosphate (STPP) were purchased from Sigma Aldrich Chemical Company. All remaining chemicals were procured from the Sigma Chemical Company, St. Louis, MO, USA, and Sisco Research Laboratory (SRL), Uttar Pradesh, India. The desired concentration of the experimental chemicals was prepared in peanut oil.

Synthesis of quercetin nanoparticles

The quercetin nanoparticles (QNP) followed the established protocol outlined by Choudhary *et al.* (2020) with minor modifications [20]. Chitosan (0.2%) was dissolved in a 2% solution of acetic acid and kept under stirring (800 rpm) overnight. Thereafter, the pH of the chitosan solution was calibrated to 4.5. Sodium tripolyphosphate (STPP) (0.2%) solution as a cross-linking agent was prepared. Thereafter the quercetin solution of 2 mg/ml concentration in ethanol was prepared and subsequently added to 10 ml of chitosan solution in a dropwise manner under magnetic stirring. The quercetin and chitosan solutions were stirred for

10 minutes, followed by the gradual addition of STPP into the quercetin-containing chitosan solution. This process occurred under a magnetic stirrer at 1200 rpm for 1 hour, leading to the creation of a translucent suspension. Moreover, the suspension underwent centrifugation at 15,000 g for 45 minutes. Following centrifugation, the liquid above the sediment was removed, and the collected pellet underwent three washes using HPLC-grade water. It was then re-suspended in HPLC-grade water and subjected to ultrasonication at 75% intensity for 10 minutes, with intervals of 10 seconds per minute. Subsequently, the sample was freeze-dried.

Characterization of quercetin nanoparticles

Determination of hydrodynamic diameter and polydispersity index (PDI) of quercetin nanoparticles

The hydrodynamic diameter and polydispersity index of the quercetin nanoparticles were assessed using a Zeta sizer from Malvern, UK. The dynamic light scattering (DLS) study was carried out to measure the hydrodynamic diameter of the quercetin nanoparticles using a zeta sizer. Briefly, the lyophilized quercetin nanoparticles were resuspended in HPLC-grade water and were subjected to DLS study, as per the manufacturer's instructions. The hydrodynamic size of the quercetin nanoparticles was measured immediately after their synthesis. Additionally, the DLS study was carried out at 60 days of synthesis to determine the stability of synthesized nanoparticles [21].

Determination of zeta potential of quercetin nanoparticles

The zeta potential of the quercetin nanoparticles was determined using the zeta sizer. The quercetin nanoparticles suspended in HPLC-grade water were injected into a cell using a syringe. The cell was then placed in the zeta sizer for the measurement of zeta potential [22].

Transmission electron microscopy (TEM) of quercetin nanoparticles

Transmission electron microscopy was done to examine the size and shape of quercetin nanoparticles. Initially, the nanoparticle suspension was applied onto a TEM grid for examination before being transferred to the microscope for imaging purposes [23].

Determination of encapsulation efficiency

Encapsulation efficiency was calculated to estimate the entrapment of quercetin nanoparticles into chitosan

nanoparticles. For this, the standard curve of quercetin was prepared to range from 0.976 to 31.25 µg/ml and the absorbance was measured at 374 nm utilizing a bio spectrophotometer from Eppendorf, Germany (Fig. 1). Following this the quercetin nanosuspension was centrifuged at 15000 g for 30 minutes and the absorbance of the supernatant was taken at 374 nm to calculate the concentration of unencapsulated/free quercetin [24]. The encapsulation efficiency was determined using the formula outlined below.

Encapsulation efficiency (%) = (Total drug-free drug) / Total drug X 100

UV-visible spectra of quercetin nanoparticles

UV Visible spectroscopy of quercetin nanoparticles was carried out to determine the storage stability of quercetin nanoparticles and to study intermolecular interaction if any, between the drug and the carrier. The absorbance of the chitosan, STPP, quercetin, and quercetin nanoparticles was taken by carrying out a full spectral scan from 250 to 600 nm. Thereafter the graph was plotted to observe the shift (Bathochromic Hypsochromic) in the peak of quercetin nanoparticles [25].

Animals and treatment

The study was carried out in adult healthy male Wistar rats, weighing approximately 120-150 g. These rats were obtained from the Laboratory Animal Resource Section at the Indian Veterinary Research Institute, Izatnagar. The animals were kept in standard housing conditions and had unrestricted access to both food and water. A nutritionally adequate standard laboratory diet was provided to animals. The daily light cycle was rotated between 12 hours of light and 12 hours of darkness. An acclimatization period of 7 days was provided before the start of the experiment. Throughout the entire study duration, continuous observation was maintained among overall experimental rats. The experimental procedures followed in this study adhered to the guidelines recommended by the Institute Animal Ethics Committee (IAEC No - 26-1/2022-23/JD(R) dated 30.07.2022) of ICAR- Indian Veterinary Research Institute and Committee for Control and Supervision of Experiments on Animals [26].

Preparation of 10% blood hemolysate

At the end of the experimental period, on the 91st day, blood samples were collected after 24 hours of fasting (feed was withdrawn but provided enough water). Blood was collected in a heparinized tube from

the retro-orbital venous plexus of the left eye and was centrifuged immediately at 3000 rpm for 10 minutes, the buffy coat and plasma layer were removed. The pellet was washed with normal saline (0.9% NaCl) three times until all the cellular debris was eliminated. The final pelleted RBCs were resuspended in sterile, double distilled water to get hemolysate [27].

Estimation of oxidative stress-related biochemical parameters

Total protein estimation in blood hemolysate (10%)

Protein was estimated by the method of Lowry *et al.* (1951) in different blood hemolysate [28]. The reaction mixture consisted of 20 µl of hemolysate, 980 µl of distilled water, 2.5 ml of alkaline copper reagent (2% sodium carbonate, 1% copper sulfate, and 2% sodium potassium tartrate) and was incubated for 10 min at room temperature. Folin-ciocalteau's reagent and shaken immediately. Afterward, the reaction mixture underwent an additional 30-minute incubation at room temperature, following which the absorbance was measured at 750 nm. BSA standards were created through sequential dilution. Subsequently, 100 µl of these standards were added to the reaction mixture to generate a standard curve by plotting concentration against OD. The obtained values were then expressed as milligrams per milliliter (mg/ml) of hemolysate.

Lipid peroxidation (LPO)

Malondialdehyde (MDA) levels, indicative of lipid peroxidation (LPO), were assessed in 10% blood hemolysate obtained from rats following a 90-day exposure to ethion, quercetin, quercetin nanoparticles, and their combination. This evaluation was conducted using the Thio-barbituric acid (TBA) method described by Shafiq-Ur-Rehman in 1984 [29]. The hemolysate (1 ml) was taken and added equal quantity of 10% w/v trichloro acetic acid, was centrifuged at 2000 rpm for 10 min. Mix 1 ml of the supernatant with an equal amount of thiobarbituric acid (0.67% w/v), then subject the mixture to a boiling water bath for 10 minutes. After cooling, dilute it with 1 ml of distilled water and measure the absorbance at 535 nm. The quantification of lipid peroxidation (LPO) is presented as the amount of moles of MDA produced per milligram of protein.

Superoxide dismutase (SOD)

SOD levels were determined following the procedure outlined by Madesh and Balasubramanian

in 1998 [30]. The mixture for the reaction comprised PBS (0.65 ml), MTT (30 μ l), Hemolysate (10 μ l, not added in control), and Pyrogallol (75 μ l). Both sample and control were incubated for 5 min at room temperature and DMSO (750 μ l) and homogenate (10 μ l to control) were added, and tubes marked as sample, blank, and control. The absorbance was measured at 570 nm against distilled water (used as the Blank). SOD activity is presented as units per milligram of protein.

Catalase (CAT)

CAT was evaluated using a spectrophotometric technique detailed by Aebi in 1983 [31]. In a test tube, 1.9 ml of phosphate buffer saline was combined with 100 μ l of hemolysate, and this mixture was subsequently transferred to a cuvette. The reaction commenced upon the addition of H₂O₂ into the cuvette. At intervals of 1 minute for 3 minutes, the optical density (OD) was measured at 240 nm against distilled water used as the blank.

Glutathione peroxidase (GPX)

GPX levels were assessed following the procedure outlined by Paglia and Valentine in 1967 [32]. The reaction mixture comprised 1.48 ml of phosphate buffer saline, along with NADPH, GSH, Sodium azide, glutathione reductase, and hemolysate. Upon adding H₂O₂ into the cuvette, the reaction commenced. The alteration in absorbance was recorded at 340 nm over a 5-minute duration.

Reduced glutathione (GSH)

GSH levels were evaluated by measuring free-SH groups utilizing 5-5' Dithio bis 2-nitrobenzoic acid (DTNB), following the procedure outlined by Sedlak and Lindsay in 1968 [33]. To 1 ml of hemolysate supernatant, 0.9 ml of distilled water and 0.1 ml of 50% TCA solution were added, and the mixture was left to incubate at room temperature for 15 minutes. Following this, the reaction mixture underwent centrifugation at 3000 g for 15 minutes. To 0.5 ml of the resulting supernatant, 0.5 ml of 1M tris buffer and 100 μ l of DTNB were added. The absorbance was measured at 512 nm within a 10-minute window.

Glutathione s-transferase (GST)

GST activity was assessed following the procedure outlined by Habig *et al.* in 1974 [34]. In a reaction mixture, 1 ml of phosphate buffer saline, 100 μ l of CDNB (1-chloro-2,4 dinitrobenzene), 100 μ l of

hemolysate, and 1.7 ml of distilled water were combined. Following an incubation period at 37°C for 5 minutes, the reaction was initiated by introducing GSH, and the absorbance was monitored at 340 nm at 1-minute intervals for 5 minutes. The outcomes were represented as the rate of CDNB-GSH conjugate formation per minute per milligram of protein.

Glutathione reductase (GR)

GR activity was evaluated using the technique described by Goldberg and Spooner in 1983 [35]. A reaction blend was prepared, containing 2.6 ml of phosphate buffer saline, 100 μ l of EDTA (15 mM), and 100 μ l of GSSG. To this mixture, 10 μ l of hemolysate was added and incubated at room temperature for 5 minutes. Subsequently, 10 μ l of NADPH was introduced, and the reduction in optical density (OD) was promptly measured for 3 minutes.

Protein carbonyl content (PCC)

PCC was evaluated following the methodology outlined by Uchida and Stadtman in 1993 [36]. The test sample contained 12.5 mM of 2, 4 - dinitrophenylhydrazine in 2 N HCl and was incubated at room temperature for 1 hour with vortexing. A 10% trichloroacetic acid was added and centrifuged at 13,000 rpm for 15 minutes at 4°C. The pellet underwent washing with 10% TCA and ethanol, followed by centrifugation at 10,000 rpm for 10 minutes. It was then dissolved in 1 ml of 6 M guanidine hydrochloride and incubated at 37°C for 30 minutes. The determination of protein carbonyl content was computed using the molar extinction coefficient of 22,000 M⁻¹cm⁻¹ at 370 nm.

Statistical analysis

Values (Mean \pm SEM, n=6) being superscripts in the same row are statistically different by two-way ANOVA followed by Tukey's post-hoc test. Comparisons were made with the control group (Arachis oil) and 1/10th LD50 group depicted as * and # respectively. The number of superscripts indicates the level of significance of p<0.033, p<0.002, and p< 0.001 with one, two, and three superscripts respectively.

RESULTS AND DISCUSSION

Characterization of quercetin nanoparticles

Hydrodynamic diameter and polydispersity index (PdI) of quercetin nanoparticles

The graphical representation of hydrodynamic diameter of quercetin nanoparticles on day 0 and day

Table 1. Different treatment groups, dose and route of administration.

Groups	Treatment	Dose / route (Oral)	Number of Rats
I	Peanut oil control	1 ml/kg	6
II	Quercetin control	50 mg/kg	6
III	Quercetin nanoparticle control	50 mg/kg	6
IV	Ethion (1/10 th LD50)	1/10 th LD50	6
V	Ethion (1/20 th LD50)	1/20 th LD50	6
VI	Ethion (1/10 th LD50) + Quercetin	II + IV	6
VII	Ethion (1/10 th LD50) + Quercetin nanoparticles	III + IV	6

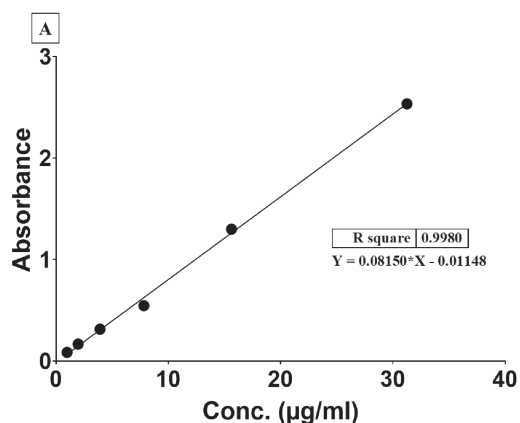
*Total experimental period was 90 days.

Table 2. Effect of ethion, quercetin and quercetin nanoparticles on oxidative stress parameters.

Treatment	Control (Arachis oil)	Control (Quercetin)	Control (NQ)	Ethion (1/10 LD50)	Ethion (1/20 LD50)	Ethion (1/10 LD50) + Quercetin	Ethion (1/10 LD50) + NQ
LPO	24.33 ^a ±0.34	24.40 ^a ±0.32	24.12 ^a ±0.29	107.30 ^d ±1.50	79.55 ^c ±0.77	47.54 ^b ±0.73	39.04 ^b ±1.39
SOD	9.33 ^a ±0.21	7.79 ^c ±1.14	9.09 ^c ±0.25	3.68 ^a ±0.07	6.37 ^b ±0.04	5.03 ^a ±0.21	6.25 ^b ±0.31
Catalase	321.73 ^d ±11.6	301.69 ^d ±10.74	319.55 ^d ±5.49	113.71 ^a ±6.94	158.18 ^b ±4.23	218.63 ^c ±6.21	234.37 ^c ±8.42
GPX	31.15 ^d ±0.86	28.46 ^d ±0.90	29.95 ^d ±0.77	9.88 ^a ±0.77	16.24 ^b ±1.63	21.03 ^c ±1.37	25.68 ^c ±1.05
GSH	0.771 ^d ±0.010	0.774 ^d ±0.017	0.767 ^d ±0.008	0.480 ^a ±0.030	0.695 ^b ±0.02	0.593 ^c ±0.008	0.715 ^d ±0.029
GST	1.110 ^c ±0.040	1.178 ^c ±0.036	1.132 ^c ±0.052	0.670 ^a ±0.033	1.065 ^b ±0.043	0.907 ^a ±0.026	1.097 ^b ±0.047
GR	30.90 ^a ±0.77	32.19 ^c ±0.94	31.79 ^c ±1.68	11.78 ^a ±0.86	21.60 ^b ±1.60	22.14 ^b ±0.63	23.66 ^b ±1.09
PCC	3.33 ^a ±0.05	3.21 ^a ±0.04	3.19 ^a ±0.04	30.91 ^c ±0.19	16.06 ^d ±0.49	13.28 ^c ±0.21	9.37 ^b ±0.25

[*LPO - Lipid Peroxidation - expressed in nmoles MDA/mg of protein. SOD - Superoxide Dismutase - expressed in Units of SOD required to inhibit the MTT reduction by 50% per gm of the protein. Catalase - expressed in nmoles of H₂O₂ utilized / min/ mg of protein. GPX- Glutathione Peroxidase - NADPH oxidized in nanomoles to NADP/min/mg protein. GSH- Reduced Glutathione - nmoles of GSH /mg protein. GST - Glutathione-S-Transferase - expressed as CDNB-GSH conjugate formed in nanomoles/min/mg protein. GR - Glutathione Reductase - nmoles of NADPH oxidized to NADP/min/mg of protein. PCC - Protein Carbonyl Content - expressed as nanomoles/mg protein.

*Values bearing superscripts are significantly different in One way ANOVA followed by Tukeys's multiple comparison test; a, b, c, d and e are the level of significance for with p<0.05. All the values are expressed in mean ± standard errors of the mean (SEM)].


Fig. 1. Graph showing standard curve of quercetin.

60 is shown in Fig. 2. The hydrodynamic size of the quercetin nanoparticles was measured immediately after their synthesis was 146±0.57 nm and the PDI was observed to be 0.21±0.01, while at day 60 of storage, the hydrodynamic diameter was found to be 165.33±0.88 nm and the PdI was 0.28±0.03.

Zeta potential and encapsulation efficiency

Fig. 3 depicts the graphical representation of the zeta potential. The zeta potential of quercetin nanoparticles on the day of synthesis was +25±1.25 mV. The same was measured for the quercetin nanoparticles at day 60 of synthesis which was found to be +32±2.35 mV and the encapsulation efficiency was found to be 92±3.59%.

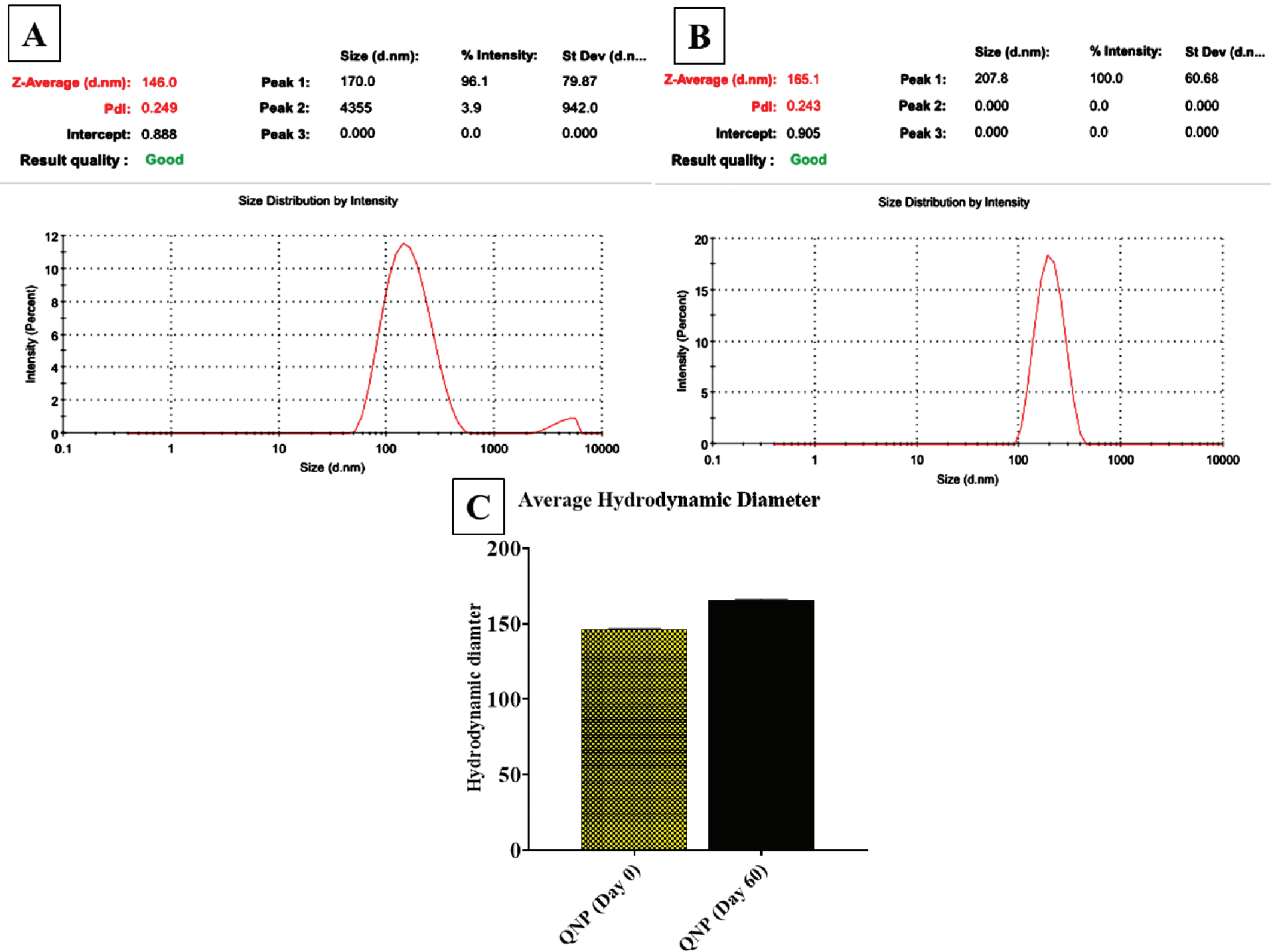


Fig. 2. (A&B): Graph generated in zeta sizer showing hydrodynamic diameter of quercetin nanoparticles at Day 0 and Day 60, respectively, (C): Graph showing hydrodynamic diameter of quercetin nanoparticles (n=3).

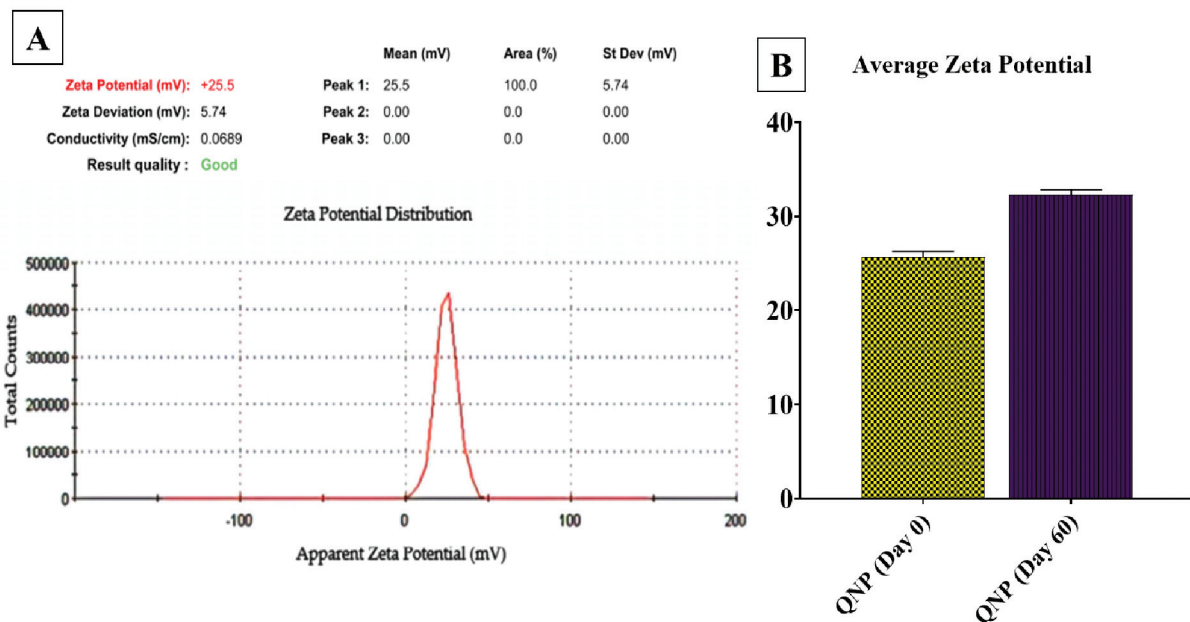


Fig. 3. (A): Graph generated in zeta sizer showing zeta potential of quercetin nanoparticles (B): Graph showing zeta potential of quercetin nanoparticles at day 0 and day 60 (n=3).

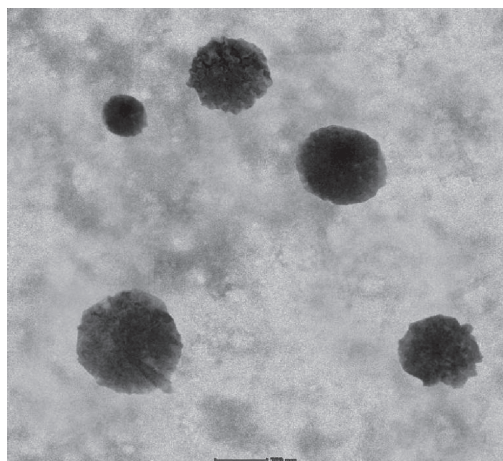


Fig. 4. TEM of quercetin nanoparticles.

TEM of quercetin nanoparticles

The representative TEM image of quercetin nanoparticles is given in Fig. 4. The scan showed that the particles were in the nano range. The TEM investigation demonstrated the spherical morphology of the quercetin nanoparticles. The size of the quercetin nanoparticles agreed with that of the hydrodynamic diameter determined using a zeta sizer, and there was no evidence of agglomeration or aggregation of the nanoparticles.

UV visible spectroscopy of quercetin nanoparticles

The quercetin showed maximum absorbance at 374 nm while the quercetin nanoparticles had maximum absorbance at 378 nm. The chitosan solution had a maximum absorbance of 231 nm and STPP showed maximum absorbance of 232 nm (Fig. 5).

Estimation of different enzymes

The oxidative enzymes, signaling pathways, and production of reactive oxygen species were all affected by quercetin's antioxidant action. The current study's findings showed a highly significant decline in the antioxidant capacities of LPO, SOD, Catalase, and GPX, as well as a significant (moderate) fall in the activity of GSH, GST, GR, and PCC respectively in animals treated with 1/10th of the LD50 of ethion. However, when compared to the control group, the LPO and catalase activity in 1/20th of the LD 50 treated animals was substantially altered. The levels of malondialdehyde in terms of LPO improved significantly after quercetin administration when combined with 1/10th of the ethion LD50, while the other parameters remained unchanged. Most of the

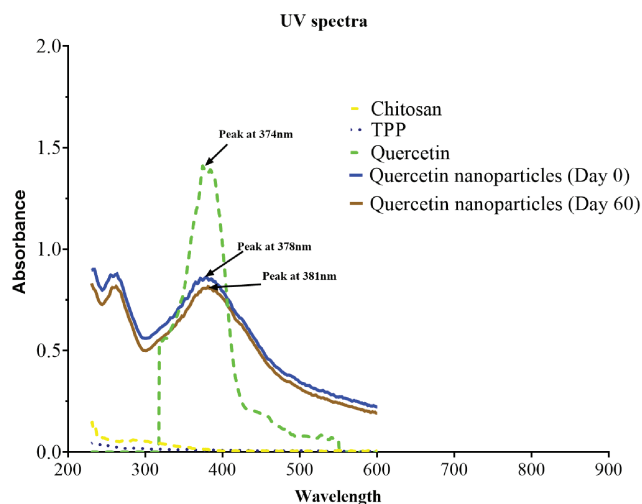


Fig. 5. UV visible spectra of quercetin nanoparticles.

oxidative stress metrics significantly (high and moderately) improved in ethion-treated animals that were exposed to quercetin nanoparticles.

The extensive use of organophosphorus insecticides due to their effectiveness and non-persistence characteristics has affected the functioning of multifarious organs/tissues of animals and humans manifesting pathological conditions [37]. The pesticide was introduced in India during the 1960s, presently it represents a common component of Indian agriculture. Organophosphates have been introduced as a substitute for organochlorine hydrocarbons due to their biodegradability. Admitting their degradation, residues are still identified in sediment, soil, and water bodies due to non-regulated usage practices. The over-dependence on pesticides has jeopardized our environment and the presence of residues in agricultural products throughout India [38].

In contemporary agricultural systems, pesticides have become a pivotal component [39]. The advent of pesticides and other technological innovations during the Green Revolution has played a significant role in enabling farmers to achieve substantial increases in crop yields, thereby contributing to enhanced food security for nations [40, 41].

Nevertheless, a prominent and widely shared objective among numerous countries and a central concern in public policy discussions is the reduction of pesticide usage. This imperative has arisen primarily due to the unequivocally demonstrated adverse effects of pesticides on both the environment and human health [42, 43]. Firstly, pesticides are recognized as one of the principal catalysts behind the decline in biodiversity, primarily resulting from the exposure of

non-target organisms within cultivated areas [44, 45, 46]. Secondly, the long-term consequences of pesticide use include the contamination of soil and water bodies due to unintended off-target movements of these chemical agents [47, 48].

Organophosphorus insecticides (OPIs) have been associated with causing oxidative stress, resulting in the creation of free radicals and changes in animals' antioxidant mechanisms. Several investigations have suggested that both enzymatic and non-enzymatic antioxidants could potentially offer protection against the toxicity induced by OPIs in humans and rats [8]. Research findings indicate that oxidative stress in biological systems arises due to an imbalance between the production of oxidizing agents and the cellular protective mechanisms provided by antioxidants [49].

The antioxidant property of quercetin is attributed to its metal-chelating ability, free radical scavenging, enzyme inhibition, and induction of repair mechanism and it substantially empowers the endogenous antioxidant shield [50]. A continued list of therapeutic agents has been discovered for oxidative damage in tissues, but a high dose is necessary to reach an acceptable therapeutic concentration at the infected tissue level [51]. Quercetin, being a potent compound, is highly hydrophobic and has negligible water solubility [52]. Due to its poor bioavailability and rapid metabolism in the body, quercetin may be less effective at preventing or treating diseases [53]. As a result, the full potential of quercetin has not been exploited. Nanotechnology offers benefits such as increasing drug absorption due to low particle size, increasing water solubility and bioavailability, decreasing risks of toxicity and degradation of drugs, and enhancing the delivery of poorly water-soluble drugs [54].

In the present study, the experiment was conducted to investigate the toxic effect of ethion at two doses and their amelioration by both quercetin and its nano-formulation in Wistar albino rats for 90 days respectively. In view of this, quercetin nanoparticles were synthesized by ionic gelation technique using chitosan and TPP [55]. The quercetin nanoparticles were characterized by investigating the hydrodynamic diameter, PdI, zeta potential, encapsulation efficiency, and UV-visible spectral analysis.

The synthesized quercetin nanoparticles were in the nano range and had a hydrodynamic diameter of 146 nm on the day of synthesis which agrees with the literature findings. To evaluate the effect of storage on the stability of quercetin nanoparticles, the lyophilized quercetin nanoparticles were stored for 60 days after

the day of synthesis and the DLS study was carried out [56].

The hydrodynamic diameter of the quercetin nanoparticles at day 60 of synthesis was found to be 165nm, which indicates that there was no significant change in the hydrodynamic diameter upon storage. The zeta potential of the quercetin nanoparticles was +25mV, which is due to the amino group in chitosan. In the present study, the encapsulation efficiency was found to be 92%, which is in agreement with the previous research. The TEM study revealed that the synthesized quercetin nanoparticles were spherical [57].

UV-visible spectroscopy was carried out to study the storage stability and intermolecular interaction. The quercetin showed a characteristic peak at 374nm while the quercetin nanoparticles had a characteristic peak at 378nm which is nearly the same as that of the quercetin, which indicates that the encapsulated quercetin had no intermolecular interaction with its carrier. Quercetin nanoparticles at day 60 also showed maximum absorbance at 381nm, thereby showing a shift in the maximum absorbance in comparison to the quercetin as well as the quercetin nanoparticles at day 0. This indicates the stability of quercetin nanoparticles at least up to 60 days of storage [58].

Reactive oxygen species (ROS) such as superoxide, hydrogen peroxide, and hydroxyl radicals, along with their reactive byproducts, are the harmful outcomes of aerobic metabolism. They possess the potential to induce DNA mutations, oxidize proteins, and trigger lipid peroxidation [59]. Multiple investigations have indicated that exposure to ethion led to elevated lipid peroxidation (LPO) and significant changes in the activities of antioxidant enzymes. These effects might arise from either a direct increase in the production of reactive oxygen species or a reduction in the cellular antioxidant capacity [9].

Malondialdehyde (MDA), an extremely reactive compound existing in the enol form, serves as a marker for lipid peroxidation (LPO) and is indicative of oxidative stress. The heightened levels of MDA seen after ethion exposure indicate an intensification of oxidative stress induced by ethion or impairment in the cellular antioxidant defenses. Similar observations of increased oxidative stress coupled with diminished antioxidant capacity were noted in the blood samples of agricultural workers exposed to organophosphorus insecticides during spraying [8].

Lipid peroxidation plays a critical role in xenobiotic toxicity, the elevation indicates the participation of free radicals-induced oxidative cell injury due to ethion

toxicity. OP compounds like dimethoate, phosphamidon, chlorpyrifos-ethyl, and ethion are reported to induce LPO in multitudinal tissues and alter diverse physiological and biochemical properties of biological systems [8]. The effect of *in vivo* administration of ethion has significantly increased the activity of LPO (in terms of MDA production) due to oxidative damage, whereas after co-administration with quercetin and quercetin nanoparticles, both have significantly normalized the oxidative stress induced by ethion.

Ethion-induced free radical damage primarily targets cellular membranes rich in vulnerable lipids susceptible to peroxidation. This oxidative damage results in the formation of stable and harmful aldehydes, such as Malondialdehyde (MDA). Notably, these aldehydes can diffuse within the cell and even traverse the plasma membrane, impacting macromolecular targets at a considerable distance from their point of origin. This phenomenon effectively renders them secondary cytotoxic messengers. Pre-treatment with quercetin nanoparticles demonstrated a pronounced reduction in MDA levels. The current body of research corroborates the robust antioxidant potential of chitosan-encapsulated nano-quercetin. This is substantiated by its ability to inhibit the generation of reactive oxygen species (ROS) and diminish the activity of MDA lipid peroxidation [15].

The major role of superoxide dismutase (SOD) is to negate the O_2^- by converting it into hydrogen peroxide (H_2O_2) by restraining the formation of highly reactive compounds like hydroxyl radical (HO) and peroxynitrite (ONOO⁻). The principle of SOD is the ability to inhibit 50% of auto-oxidation of pyrogallol [60]. Catalase and heme-containing enzyme mediates the Dismutation of H_2O_2 to H_2O and O_2 . The turnover conversion rate is very high as 6×10^6 molecules of H_2O_2 are converted to H_2O and O_2 and do not require a reducing equivalent [61]. Glutathione (GSH) is derived from three amino acids *i.e.*, glutamate, glycine, and cysteine with a tripeptide bond. GSH exists in two states *i.e.*, reduced (GSH) and oxidized (GSSG) [62]. Glutathione peroxidase (GPX) catalyzes the reduction of HO_2 and H_2O_2 to lipid alcohols and water, its activity has been implied as a biomarker for intracellular oxidative stress and their activity will be at maximal during biotic and abiotic stress [63, 64].

Glutathione-S-transferase initiates the nucleophilic assault on the sulfur atom of glutathione and exhibits remarkable versatility, accommodating numerous substrates across a broad spectrum of reactions [65, 66, 67]. Carbonyl groups, comprising aldehydes and ketones, are generated on the side chains of proteins

during oxidation. This process occurs through oxidative cleavage, either via the amidation pathway or through the oxidation of the glutamyl side chain. This results in the creation of a peptide N-terminal (amino acid) that is blocked by an alpha-ketoacyl derivative [68]. Protein carbonyl groups are frequently employed as biomarkers for peroxidation due to their early formation and stability in oxidized proteins, which can persist for hours to days. This contrasts with lipid peroxide products, which exhibit a shorter lifespan, typically lasting only minutes [69]. The use of nano-quercetin has shown a significant increase in the functions of key antioxidants, including glutathione (GSH), glutathione peroxidase (GPx), superoxide dismutase (SOD), and glutathione S-transferase (GST). This improvement stands out, especially in its ability to alleviate ethion-induced toxicity [70]. This emphasizes its function in counteracting the harmful impacts of oxidative stress. Remarkably, nano-quercetin exhibits significant hemoprotective characteristics, clearly demonstrated through its antioxidant capabilities [71]. These findings highlight the strong therapeutic promise of nano-quercetin in safeguarding against oxidative damage and the related health consequences.

In the present study, a concentration-dependent and significant decrease in SOD, Catalase, GSH, GPX, GST, and GR in ethion-treated animals and an increase in protein carbonyl content, following the administration of quercetin and quercetin nanoparticles, the extent of oxidative stress and its biomarkers has been significantly improved especially in quercetin nanoparticles group.

CONCLUSION

The outcomes of this study suggest that rat exposure to ethion leads to the onset of oxidative stress, as assessed by parameters including lipid peroxidation (LPO), superoxide dismutase (SOD), catalase, glutathione (GSH), glutathione peroxidase (GPX), glutathione reductase (GR), and protein carbonyl content. The results showed an increase in the oxidative stress parameters. Concurrent administration of quercetin and quercetin nanoparticles ameliorated the effect of ethion-induced oxidation due to their anti-inflammatory and antioxidant activity in rats.

ACKNOWLEDGMENT

All the authors are highly thankful to the administration of ICAR-Indian Veterinary Research Institute, Bareilly, U.P, India, for providing essential facilities and support for carrying out the present study.

REFERENCES

1. Loza MMA, Juan RS, Juan FST. *In silico* studies on compounds derived from *Calceolaria*: Phenylethanoid glycosides as potential multitarget inhibitors for the development of pesticides. *Biomol.* 2018; 121(8): 1-16.
2. Panagiotakopulu E, Buckland PC, Day PM. Natural insecticides and insect repellents in antiquity: a review of the evidence. *J Archeol Sci.* 1995; 22(5): 705-710.
3. Hassan AG, Soliman M, Hamdy Taha, Sayed AMA, Monira A *et al.* Pathogenic effects of ethion residues and the expected protective role of the ethanolic extract of Rosemary (*Rosmarinus officinalis* L.) leaves in male rats. *Egypt J Chem.* 2021; 64(4): 1817-1829.
4. Singh M, Sandhir R, Kiran R. Erythrocyte antioxidant enzymes in toxicological evaluation of commonly used organophosphate pesticides. *Ind J Exp Biol.* 2006; 44(7): 580-583.
5. EPA (Environmental Protection Agency). Guidance for the reregistration of pesticide products containing thephos as the active ingredient. 1998; Washington DC.
6. Abdel GH, Taha H, Sayed MA. Ameliorative effect of rosemary extract (*Rosmarinus Officinalis* L.) against ethion bound residues induced alterations in experimental animals. *Adv in Agri Tech Pl Sc.* 2020; 3(1): 1-10.
7. Abdel HRM, Taha M, Abdel GH, Mahdy F, Hegazi B. Zeolitic imidazolate frameworks: Experimental and molecular simulation studies for efficient capture of pesticides from wastewater. *J Environ Chem Eng.* 2019; 7(6): 103499.
8. Bhatti GK, Kiran R, Sandhir R. Modulation of ethion-induced hepatotoxicity and oxidative stress by vitamin E supplementation in male Wistar rats. *Pest Biochem Physio.* 2010; 98(1): 26-32.
9. Bhatti GK, Bhatti JS, Kiran R, Sandhir R. Biochemical and morphological perturbations in rat erythrocytes exposed to ethion: protective effect of vitamin E. *Cell Mol Bio.* 2011; 57(1): 70-79.
10. Hou Y, Zeng Y, Li S, Lei Q, Xu W. Effect of quercetin against dichlorvos induced nephrotoxicity in rats. *Exp Toxicol Pathol.* 2014; 66(4): 211-218.
11. Ozyurt H, Cevik O, Ozgen Z, Ozden S, Cadraci MA *et al.* Quercetin protects radiation induced DNA damage and apoptosis in kidney and bladder tissues of rats. *Free Radic Res.* 2014; 48(10): 1247-1255.
12. Uzun FG, Demir F, Kalender S, Bas H, Kalender Y. Protective effect of catechin and quercetin on chlorpyrifos-induced lung toxicity in male rats. *Food Chem Toxicol.* 2010; 48(6): 1714-1720.
13. Ghosh S, Ddungdung SR, Chowdhury ST, Mandal AK, Sarkar S *et al.* Encapsulation of the flavonoid quercetin with an arsenic chelator into nano capsules enables the simultaneous delivery of hydrophobic and hydrophilic drugs with a synergistic effect against chronic arsenic accumulation and oxidative stress. *Free Radi Bio Med.* 2011; 51(10): 1893-1902.
14. Gelperina S, Kisich K, Iseman MD, Heifets L. The potential advantages of nanoparticle drug delivery systems in chemotherapy of tuberculosis. *Am J Resp Cri Care Med.* 2005; 172(12): 1487-1490.
15. Gupta V, Kant V, Sharma M. Synthesis and *in vitro* assessment of zinc oxide nanoparticles for their antioxidant and antibacterial potentials. *Explor Anim Med Res.* 2020; 10(2): 124-133.
16. Gupta V, Prasad R, Singh P, Kant V, Kumar P, Sharma M. Synthesis and characterization of copper oxide nanoparticles and their cutaneous wound healing potential. *Explor Anim Med Res.* 2020; 10(2): 188-194.
17. Paul A, Sujatha K. Concurrent effect of *Linum usitatissimum* and *Emblica officinalis* on lead induced oxidative stress and histomorphological changes in uterus of female Wistar rats. *Explor Anim Med Res.* 2022; 2(2): 264-272.
18. Pattanayak S. Anti-COVID-19 biomedicines - a layout proposal for production, storage and transportation. *The Open COVID J* 2021; 1: 166-188.
19. Pattanayak S. Anti-cancer plants and their therapeutic use as succulent biomedicine capsules. *Explor Anim Med Res.* 2023; 13(Ethnomed. Spl.): 01-50.
20. Choudhary A, Vinay K, Jangir BL, Joshi VG. Quercetin loaded chitosan tripolyphosphate nanoparticles accelerated cutaneous wound healing in Wistar rats. *Eur J Pharmacol* 2020; 880: 173172.
21. Hassani SA, Laouini H, Fessi CC. Preparation of chitosan-TPP nanoparticles using microengineered membranes; Effect of parameters and encapsulation of tacrine. *Colloids and surfaces A: Physicochem Eng Asp.* 2015; 1345(7): 159-168.
22. Hunter R, Midmore HZ. Zeta potential of highly charged thin double-layer systems. *J Colloid Interf Sci.* 2001; 237: 147-149.
23. Nan W, Ding L, Chen H, Khan FU, Yu L *et al.* Topical use of quercetin-loaded chitosan nanoparticles against ultraviolet B radiation. *Front Pharmacol.* 2018; 9: 826.
24. Laouini A, Koutroumanis KP, Charcosset SC, Georgiadou H, Fessi RG *et al.* pH-sensitive micelles for targeted drug delivery prepared using a novel membrane

contactor method, ACS Appl Mat Interfaces. 2013; 5: 8939-8947.

25. Kain D, Kumar S. Synthesis and characterization of chitosan nanoparticles of *Achillea millefolium* L. and their activities. F 1000 Research. 2020; 9: 1297(1-14).

26. CCSEA (Committee for the Purpose of Control and Supervision of Experiments on Animals. 2003 amended via S.O 933(E) dated 21.06.2006. https://cpcsea.nic.in/WriteReadData/userfiles/file/SOP_CPCSEA_inner_page.pdf. Accessed on 25.10.2022.

27. Robert JA, Carla JR, Thomas JB. Human red blood cell hemolysate is a potent mitogen for renal tubular epithelial cells. Renal Failure. 2000; 22(3): 267-281.

28. Lowry OH, Rosebrough NJ, Farr AL, Randall RJ. Protein measurement with the Folin phenol reagent. J Biol Chem. 1951; 193(1): 265-275.

29. Shafiq-Ur-Rehman. Lead-induced regional lipid peroxidation in brain. Toxicol Letters. 1984; 21: 333-337.

30. Madesh M, Balasubramanian KA. Microtiter plate assay for superoxide dismutase using MTT reduction by superoxide. Ind J Biochem Biophys. 1998; 35: 184-188.

31. Aebi HE. Catalase *in vitro*. Mthds Enzymol. 1983; 105: 121-126.

32. Paglia DE, Valentine WN. Studies on the quantitative and qualitative characterization of erythrocyte glutathione peroxidase. J Lab Clin Med. 1967; 70(1): 158-169.

33. Sedlak J, Lindsay RH. Estimation of total, protein-bound, and non-protein sulfhydryl groups in tissue with Ellman's reagent. Anal Biochem. 1958; 24(2): 192-205.

34. Habig WH, Pabst MJ, Jakoby WB. Glutathione S-transferases : The first enzymatic step in mercapturic acid formation. J Biol Chem. 1974; 249(22): 7130-7139.

35. Goldberg DM, Spooner RJ. Glutathione reductase. In: Methods of enzymatic analysis, Weinheim, Germany. 1983; 3(3): 258-265.

36. Uchida K, Stadtman ER. Covalent attachment of 4-hydroxynonenal to glyceraldehydes-3-phosphate dehydrogenase. J Biol Chem. 1993; 268(9): 6388-6393.

37. Worek FT, Wille M, Thiermann KH. Toxicology of organophosphorus compounds in view of an increasing terrorist threat. Arch of Tox. 2016; 90(5): 2131-2145.

38. Kumar S, Garima K, Juan FV. Scenario of organophosphate pollution and toxicity in India: A review. Environ Sci Pollut Res Int. 2016; 23(10): 9480-9491.

39. Popp J, Peto K, Nagy J. Pesticide productivity and food security: A review. Agron Sustain Dev. 2013; 33: 243-255.

40. Cooper J, Dobson H. The benefits of pesticides to mankind and the environment. Crop Prot. 2007; 26: 1337-1348.

41. Hedlund J, Longo S, York R. Agriculture, pesticide use, and economic development: a global examination (1990-2014). Rural Sociol. 2019; 85: 5190-544.

42. Barzman M, Dachbrodt SS. Comparative analysis of pesticide action plans in five European countries. Pest Manag Sci. 2011; 67: 1481-1485.

43. Lee R, den UR, Runhaar H. Assessment of policy instruments for pesticide use reduction in Europe; learning from a systematic literature review. Crop Prot. 2019; 126: 104929.

44. Geiger F, Bengtsson J, Berendse F *et al*. Persistent negative effects of pesticides on biodiversity and biological control potential on European farmland. Basic Appl Ecol. 2010; 11: 97-105.

45. IPBES. Assessment report on pollinators, pollination and food production. Inter-governmental Science-Policy Platform on Biodiversity and Ecosystem Services, Bonn, Germany. 2016. <https://www.ipbes.net/assessment-reports/pollinators>. Accessed on 26.10.2023.

46. Sanchez BF, Wyckhuys KAG. Worldwide decline of the entomofauna: a review of its drivers. Biol Conserv. 2019; 232: 8-27.

47. Pietrzak D, Kania J, Malina G *et al*. Pesticides from the EU first and second watch lists in the water environment. CLEAN Soil Air Water. 2019; 47: 1800376.

48. Pelosi C, Bertrand C, Daniele G *et al*. Residues of currently used pesticides in soils and earthworms: a silent threat? Agric Ecosys Environ. 2021; 305: 107167.

49. Tuzmen N, Candan N, Kaya E, Demiryas N. Biochemical effects of chlorpyrifos and deltamethrin on altered antioxidative defense mechanisms and lipid peroxidation in rat liver. Cell Biochem Funct. 2008; 26(1): 119-124.

50. Boots AW, Guido RM, Haenen M, Aalt B. Health effects of quercetin: From antioxidant to nutraceutical. Eur J Pharmacol. 2008; 585(2-3): 325-337.

51. Ghosh A, Ardhendu KM, Sibani S, Subhamay P, Das N. Nanoencapsulation of quercetin enhances its dietary efficacy in combating arsenic-induced oxidative damage in liver and brain of rats. Life Sci. 2009; 84(3-4): 75-80.

52. Srinivas K, King JW, Howard LR, Monrad JK. Solubility and solution thermodynamic properties of quercetin and quercetin dihydrate in subcritical water. *J Food Eng.* 2010; 100(2): 208-218.
53. Oboh G, Ademosun AO, Ogunsuyi OB. Quercetin and its role in chronic diseases. *Adv Exp Med Biol.* 2016; 929: 377-387.
54. Emeje MO, Ifeoma CO, Ekaete IA, Sabinus IO. Nanotechnology in Drug Delivery, ISBN- 978-953-51-4268-3. 2012; 514.
55. Terron MK, Benavidez EM, Ciapara IA, Virues C, Hernández J *et al.* Mesoscopic modeling of the encapsulation of capsaicin by lecithin/chitosan liposomal nanoparticles. *Nanomaterials.* 2018; 8: 425.
56. Senyigit TF, Sonvico A, Tekmen RI, Santi P, Colombo P *et al.* *In vivo* assessment of clobetasol propionate-loaded lecithin-chitosan nanoparticles for skin delivery, *Int J Mol Sci.* 2016; 18: 32.
57. Rashedi J, Ghorbani HA, Mesgari AM, Dastranj TA, Yaqoubi S *et al.* Anti-tumor effect of quercetin loaded chitosan nanoparticles on induced colon cancer in Wistar rats. *Adv Pharmaceut Bulletin.* 2019; 9(3): 409-415.
58. Johra FT, Sukria H, Preeti J, Bristy AT, Emran T *et al.* Amelioration of CCl₄-induced oxidative stress and hepatotoxicity by *Ganoderma lucidum* in Long Evans rats. *Scientific Reports.* 2023; 13: 9909.
59. Mirshafiey A, Mohsenzadegan M. The role of reactive oxygen species in immunopathogenesis of rheumatoid arthritis. *Iran J Allergy Asthma Immunol.* 2008; 7(4): 195-202.
60. Mohamad EA, Manal AAK, Elsalawy AM, Hazaa SM. Assessment of lipid peroxidation and antioxidant status in rheumatoid arthritis and osteoarthritis patients. *Egyptian Rheumatologist.* 2011; 33(4): 179-185.
61. Afonso V, Champy R, Mitrovic D, Collin P, Lomri A. Reactive oxygen species and superoxide dismutases: role in joint diseases. *Joint Bone Spine.* 2007; 74(4): 324-329.
62. Mittler R. Oxidative stress, antioxidants and stress tolerance. *Trends Plant Sci.* 2002; 7(9): 405-410.
63. Zhou Y, Hu L, Ye S, Jiang L, Liu S. Genome-wide identification of glutathione peroxidase (GPX) gene family and their response to abiotic stress in cucumber. 2018; *Biotech* 8(3): 159.
64. Wang Z, Tang SF, Hou X. Glutathione peroxidase 6 from *Arabidopsis thaliana* as potential biomarker for plants exposure assessment to di-(2-ethylhexyl) phthalate. *Spectrochim Acta Part A Mol Biomol Spectrosci.* 2020; 229: 117955.
65. Vaish S, Gupta D, Mehrotra R, Mehrotra S, Basantani MK. Glutathione s-transferase: A versatile protein family. 2020; 3-Biotech. 10(7): 321.
66. Hernandez Estevez I, Rodríguez Hernández M. Plant glutathione s-transferases: An overview. *Plant Gene.* 2020; 23: 100233.
67. Hou X, Tan L, Tang SF. Molecular mechanism study on the interactions of cadmium (II) ions with *Arabidopsis thaliana* glutathione transferase Phi8. *Spectrochim Acta Part A Mol Biomol Spectrosc.* 2019; 216: 411-417.
68. Berlett BS, Stadtman ER. Protein oxidation in aging, disease, and oxidative stress. *J Biol Chem.* 1997; 272(33): 20313-20316.
69. Siems WG, Zollner H, Grune T, Esterbauer H. Metabolic fate of 4-hydroxynonenal in hepatocytes: 1,4-dihydroxynonenone is not the main product. *J Lipid Res.* 1997; 38(3): 612-622.
70. Ibrahim SS, Barakat MA, Helmy H. Modulating effect of carvedilol on doxorubicin-induced cardiomyopathy and hepatic damage. *J Am Sci.* 2010; 6(12): 20-32.
71. Raj LFAA, Jonisha R, Revathi B, Jayalakshmy E. Preparation and characterization of BSA and chitosan nanoparticles for sustainable delivery system for quercetin. *J Appl Pharm Sci.* 2015; 5(7): 001-005.

Cite this article as: Ranjith D, Kamothi DJ, Madhu CL, Padhi PK, Dinesh Kumar, Telang AG. Synthesis, characterization and ameliorating effect of quercetin nanoparticles against ethion-induced oxidative stress in male rats. *Explor Anim Med Res.* 2023; 13(2), DOI: 10.52635/eamr/13.2.231-242.